African Journal of Biotechnology Vol. 10(78), pp. 17925-17933, 7 December, 2011
Available online at http://www.academicjournals.org/AJB
DOI: 10.5897/AJB11.1271
ISSN 1684–5315 © 2011 Academic Journals

Full Length Research Paper

Cloning, expression and functional analysis of MAP30 from *Momordica charantia* reveals its induction of apoptosis of the BGC-823 cells

Xiao-Hong Han[1], Yan-Jun Xue[2], De-yu Chen[3], Shi-He Shao[4]*, He Huang[5], Xian-Qian Li[6] and Hua-Xi Xu[7]

[1]Department of Pathology, School of Medical Science and Laboratory Medicine of Jiangsu University, Zhenjiang, 212013, Jiangsu, P. R. China.
[2]Department of Human Anatomy, School of Medical Science and Laboratory Medicine of Jiangsu University, Zhenjiang, 212013, Jiangsu, P. R. China.
[3]Department of Oncology, Affiliated Hospital of Jiangsu University, Zhenjiang, 212000, Jiangsu, P. R. China.
[4]Department of Microbiology, School of Medical Science and Laboratory Medicine of Jiangsu University, Zhenjiang, 212013, Jiangsu, P. R. China.
[5]Institute for Life Sciences of Jiangsu University, Zhenjiang, 212013, Jiangsu, P. R. China.
[6]Laboratory of Cancer, Putuo Hospital affiliated to Shanghai University of Traditional Chinese Medicine, Shanghai, 200062, P. R. China.
[7]Institute of Clinical Laboratory Medicine of Jiangsu University, Zhenjiang, 212013, Jiangsu, P. R. China.

Accepted 15 July, 2011

Momordica Anti-HIV Protein 30 (MAP30) can induce many tumour cells apoptosis, but the mechanism is still unclear. Since the content of MAP30 in *Momordica charantia* is limited, in this study, the MAP30 gene was cloned and expressed and the induction of the recombinant MAP30 protein on the apoptosis of BGC-823 cells was investigated. Morphological changes were observed by microscopy. The normal, apoptotic and necrotic cells were identified by fluorescence staining. The apoptosis percentage and the mitochondria membrane potential level was displayed by flow cytometry analysis and JC-1 fluorescent probe assay, respectively. The mRNA expression of caspase-9 and Apaf-1 was investigated by reverse transcription polymerase chain reaction (RT-PCR). The content of Cyt C and the activity of Caspase-3 were investigated by ELISA and spectrophotometric method, respectively. In this study, the MAP30 gene was expressed and the recombinant MAP30 protein was purified successfully. The results of morphology, the fluorescence staining and the flow cytometry analysis indicated that MAP30 could induce cells apoptosis. When treated with MAP30, the mitochondria membrane potential level decreased, while the expression of caspase-9 and Apaf-1 mRNA, the Cyt C content, and the caspase-3 activity all increased. All these indicated that the recombinant MAP30 protein could induce the BGC-823 cells apoptosis *in vitro* via the mitochondrial pathway.

Key words: *Momordica charantia*, MAP30, BGC-823 cells, apoptosis, mitochondria membrane potential, Cyt C, caspase-9, Apaf-1, caspase-3.

INTRODUCTION

Momordica charantia (MC), a member of the Cucurbitaceae family, grows in tropical areas and is used traditionally as both food and medicine. It contains many active constituents which are currently used in the treatment of diabetes, dyslipidemia and microbial infections, and considered as potentially cytotoxic agents for certain types of cancer (Anonymous, 2007). MAP 30

*Corresponding author. E-mail: Shaoshihe2006@163.com.

Abbreviation: MC, *Momordica charantia.*

isolated from MC is a kind of type-I ribosome inactivating protein (RIP) and can induce the apoptosis of tumor or the viral infected cells (Lee-Huang et al., 2000), but the content of natural MAP30 in MC is limited, technology of extraction is complex and output is rather low. Several studies have demonstrated that the antiviral and anti-tumor activities of MAP30 are independent of their ribosome inactivation activity (Huang et al., 1999). Thus, recombinant expressed MAP30 exhibits comparable antiviral, anti-tumor and antimicrobial activities as their counterparts from their original plant sources (Arazi et al., 2002). In this study, therefore, the MAP30 gene was cloned and expressed, and the apoptosis-inducing function of the recombinant MAP30 protein on BGC-823 cells was investigated.

MAP30 has a variety of biological activities, one of which is specific to tumor-transformed or viral-infected cells (Lee-Huang et al., 2000). It shows no adverse effects on normal cells such as human normal cells, T cells, diploid cells and sperm cells (Lee-Huang et al., 1995; Schreiber et al., 1999), making it a candidate for clinical applications. Although, it has been shown that MAP30 could induce apoptosis in human breast tumor (Lee-Huang et al., 2000), little is known about its effects on gastric carcinoma. The gastric carcinoma is one of the most common malignant tumors worldwide, so this study was aimed at investigating whether MAP30 could induce the human gastric carcinoma BGC-823 cells apoptosis and the apoptosis mechanism was further study. Our results show that the recombinant MAP30 could induce the BGC-823 cell apoptosis via mitochondria-mediated pathway.

MATERIALS AND METHODS

Preparation of the recombinant MAP30

The genome DNA was extracted from the fresh leaves of MC by cetyltrimethyl ammonium bromide (CTAB). Polymerase chain reaction (PCR) was used to amplify the MAP30 gene from genome DNA. Then, the target gene was inserted into the vector pGEM-T (Progema, USA). The pGEM-T-MAP30 vector was transformed into *Escherichia coli* DH5α and identified by restriction digestion and DNA sequencing. Then, the MAP30 gene fragment was inserted directionally into expression vector pET-28a (Novagen Ltd, USA). The pET-28a-MAP30 expression vector was transformed into *E. coli* BL21 (DE3). The his-MAP30 fusion protein was expressed in *E. coli* BL21 (DE3) induced by Isopropylthio-β-D-galacgoside (IPTG). The target fusion protein was purified by Ni^{2+}-NTA columns and identified by SDS-PAGE through gray scale scanning by a Gel Doc 2000 gel image analysis system (Bio-Red, USA).

Cell culture

The human gastric carcinoma BGC-823 cells (ATCC Number: CRL-1739, Cell Bank of Science Academy, China) were provided by Prof. Shi-He Shao (Jiangsu University, Zhenjiang, China). Cells were grown in culture at 37°C and 5% CO_2 in RPMI medium 1640 (Gibco, USA) supplemented with 10% fetal bovine serum (Beyotime Institute of Biotechnology, Shanghai, China).

Morphological observation

For observation using light microscopy, cells were treated with 30 µg/ml MAP30 for 48 h. The control group was given only culture medium containing no drugs. Each treatment was tested in tetrad flasks. Morphological changes were observed under light microscope. For observation with electron microscopy, cells were cultured with 30 µg/ml MAP30 for 48 h. The control group was given only culture medium containing no drug. Each treatment was tested in tetrad flasks. The cells were collected and then fixed with 2% paraformaldehyde / 2% glutaraldehyde in 0.1 mol/L phosphate buffer (pH 7.4), followed by 1% osmium tetroxide. After dehydration, thin sections were stained with uranyl acetate and lead citrate for observation under a JEM 2000 EX electronmicroscope (JEC, USA).

Identification of normal, apoptotic and necrotic cell by fluorescence staining

The identification of normal, apoptotic and necrotic cell was carried out using a Normal/Apoptotic/Necrotic cell Detection Kit (NANJING KEYGEN BIOTECH. CO., LTD) according to the manufacturer's instruction. The cells were treated with 30 µg/ml MAP30 for 48 h. The control group was given only culture medium containing no drug. Each treatment was tested in tetrad flasks. Cells were observed under a fluorescence microscope equipped with a 510 nm excitation filter and photos were taken by a Nikon eclipse TE300 and Nikon Digital Sight (Nikon, JAPAN). The cells apoptotic/necrotic efficiency was calculated according to the following formula: cells apoptotic efficiency (%) = (nonage apoptotic cells + advanced stage apoptotic cells) / cell number × 100; cells necrotic efficiency (%) = necrotic cells/cell number × 100.

Flow cytometric analysis

Cellular DNA content and cell distribution were quantified by flow cytometer (FCM) using propidium iodide (PI) (Sigma, USA). The cells were treated with 30 µg/ml MAP30 for 12, 24 and 48 h, respectively. The control group was given only culture medium containing no drug. Each treatment was tested in tetrad flasks. The cells (1×10^6) were collected and fixed in 70% alcohol at 4°C overnight, the cells were then centrifuged for five minutes at 1000 rpm. The supernatant was removed and the cells were washed twice with PBS. Then, the cells were resuspended in 3 ml PBS and 3 ml phosphate-citrate buffer (0.2 M Na_2HPO_4 and 0.1 M citric acid) was added to the cells. After 30 min incubation, cells were collected and resuspended in 150 µl PI and 200 µl RNaseA (Sigma, USA). The samples were incubated at room temperature in the dark for 30 min and analyzed by a FACS 420 FCM (Becton Dickinson Co., USA) in triplicate. Cell populations in the sub-G1 area were quantified from a standard count of 10^4 cells using MULTYCYCLE software (PHEONIX Co., USA).

Evaluation of mitochondrial membrane potential ($\Delta\Psi_m$)

The $\Delta\Psi_m$ of the cells was investigated by a mitochondrial membrane potential assay kit with JC-1 (BioVision, Inc., USA) according to the manufacturer's instruction. Cells were seeded into 24-well plates (7×10^4/ml) and 30 µg/ml MAP30 was added into treated wells 24 h later. Only culture medium containing no drugs was added to the negative control wells. Carbonylcyanide-m-chlorophenylhydrazone (CCCP) was added to the positive control wells. ach treatment was tested in tetrad wells. All the plates were incubated for 6, 12, 24 and 48 h, respectively. Expressions of JC-1 J-aggregates and JC-1 monomers were observed under a fluorescence microscope and photos were taken by a Nikon eclipse

TE300 and Nikon Digital Sight (Nikon, Japan).

Determination of Cyt C concentration in cell's supernatant

Cyt C concentration in cell's supernatant was assayed by the Human Cytochrome-C Enzyme Linked Immunosorbent Assay Kit (R&D Co., USA) according to the manufacturer's instruction. The BGC-823 cells were plated in 96-well plates (8×10^4/ml) and allowed to attach overnight. The cells were treated with MAP30 (25 and 50 µg/ml) for 6, 12, 24, 48 and 72 h, respectively. The control group was given only culture medium containing no drug. Each treatment was tested in tetrad wells. Samples were read in a Microplate Fluorescence Reader (SPECTRA MAX GEMINI EM, Molecular Devices, USA) equipped with a 450 nm wavelength.

Expressions of caspase9 and Apaf1 mRNA

Gene expression was analyzed by reverse transcription polymerase chain reaction (RT-PCR) procedure. The extraction of RNA was performed by RNA Extraction Kit (Fastagen Inc, China) and the RNA reverse transcription was carried out by RevertAid™ First Strand cDNA Synthesis Kit (Fermentas Inc, Canada). Total RNA was extracted from BGC-823 cells treated with 30 µg/ml MAP30 for 24, 48 and 72 h, respectively, and negative control cells using Fastagen reagent according to the manufacturer's instructions. cDNA was synthesized from 1 µg of total RNA using ReverTra Ace (Fermentas Inc, Canada) according to the manufacturers' instructions. The following primers were used: caspase9, forward 5′-CAGAAAGACCATGGGTTTGAG-3′ and reverse 5′-ACTGCAGGTCTTCAGAGTGAG-3′; Apaf1, forward 5′-ATGAGAGTTTTTCC- CAGAGGCTTC-3′ and reverse 5′-TTGAGGTAGTACTCCCAGCGATTG-3′; GAPDH, forward 5′-AACGGATTTGGTCGTATTGGG-3′ and reverse 5′-TCGCTCCTGGAAGATGGTGAT-3′. Quantitative RT-PCR was conducted in 0.5 µM of each set of primers in 20 µl final reaction volume of Premix Ex Taq™ (Takara Bio Inc, Japan), PCR cycling conditions were as follows: 95°C for 30 s and 40 cycles of 95°C for 5 s, 60°C for 20 s and 70°C for 30 s. The calculated concentration was normalized to the expression level of GAPDH mRNA. All qRT-PCR reactions were performed in duplicate, and repeated three times.

Determination of caspase-3 activity

Caspase-3 activity was assayed by the Caspase-3 Colorimetric Assay Kit (NANJING KEYGEN BIOTECH. CO., LTD) according to the manufacturer's instructions. The BGC-823 cells were plated in 50 ml culture flasks (1×10^6 cells/flask) and allowed to attach overnight. The cells were treated with MAP30 (25 and 50 µg/ml) for 6, 12, 24 and 48 h, respectively. The control group was given only culture medium containing no drug. Each treatment was tested in tetrad flasks. Samples were read in a Microplate Fluorescence Reader (SPECTRA MAX GEMINI EM, Molecular Devices, USA) equipped with a 400 nm wavelength.

Caspase-3 activity = $OD_{MAP30}/OD_{control}$

Statistical analysis

Data were given as the means ± SD. Variance analysis between groups was performed by one-way ANOVA and significance of difference between control and treatment groups was analyzed using *t*-test. The differences with $p<0.05$ were considered statistically significant.

RESULTS AND DISCUSSION

The cloning and expression of MAP30 gene

DNA sequence analysis showed that the sequence of MAP30 was 861 bp. It has homology with DQ643967, DQ643968 and S79450. The prokaryotic expression vector pET-28a-MAP30 was transformed into *E. coli* BL21 (DE3) efficiently. The fusion protein was expressed at 30°C after 0.5 mmol/L IPTG induction for 5 h (Figures 1 and 2). The protein was purified using NTA-Ni-Charged Resin affinity column conveniently, the purity was above 90% by SDS-PAGE assay, which is shown in Figure 2, and its relative molecular weight was 30 kDa. This indicates that the fusion protein MAP30 was obtained from *E. coli* BL21 (DE3) successfully.

Induction of the apoptosis of BGC-823 cells

Apoptosis is a central regulator of normal tissue homeostasis. Disturbed apoptosis is involved in the pathogenesis of multiple diseases, especially of cancer. Consequently, the induction of apoptosis on the anticancer strategies has been emphasized (Fulda and Debatin, 2006). Apoptosis is characterized by its specific morphological features and the morphological changes usually involves: Cells shrink, cytoplasm pycnosis, karyosome disappears, the nuclear chromatin is condensed and aggregates peripherally, under the nuclear membrane into well-delimited masses of various shapes and sizes; nuclear membrane twisting, sometimes crescentic cap form, and at the end the apoptotic bodies development. In this study, when treated with MAP30, some cells became round, blunt and shrink, smaller in size, had membrane blebbing, holes, cytoplasmic extrusions and formation of apoptotic bodies under light microscope (Figure 3). The ultrastructural and morphological changes in BGC-823 cells were observed under electron microscope: the microvilli on the surface of the cells disappeared, there was cells shrink, cytoplasm pycnosis, nuclear membrane fold and twist, nuclear condensation, nuclear chromatin agglutination, and condensed to lump and close to membrane (Figure 4). Furthermore, the fluorescence staining confirmed that MAP30 could induce the BGC-823 cells apoptosis meanwhile the normal, apoptotic and necrotic cells were identified. The fluorescence staining indicated that MAP30 could induce the BGC-823 cells apoptosis, and the apoptotic efficiencies (%) of the control and MAP30 treated groups were 0.418 ± 1.025% and 25.3 ± 2.132%, respectively (MAP30 treated group $p<0.01$ vs. control group). As shown in Figure 5, FCM with only PI staining showed that the subdiploid nuclear peak appeared on the left side of G1 peak when the cells were treated with MAP30, and the apoptotic efficiencies (%) of the control, 12, 24 and 48 h treatment groups were 6.19, 8.73, 10.35

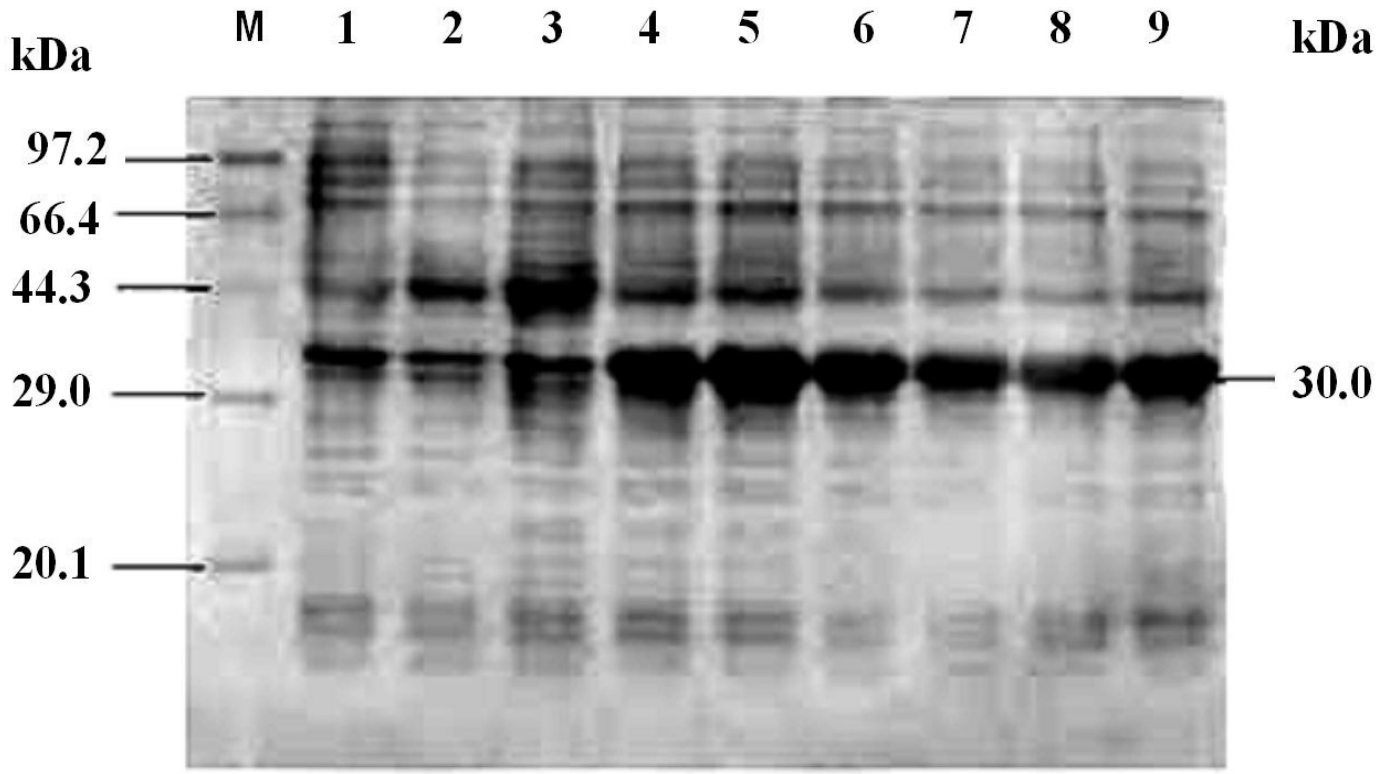

Figure 1. The effect of inducing concentration on the expression amount of recombinant MAP30. Expression of 6×His-tagged MAP30 protein was induced by different concentrations of IPTG for 4 h. M, Marker; lane 1, negative control (BL21(DE3)); lane 2, negative control (pET-28a/ BL21(DE3)); lanes 3 to 9, induced by 0, 0.3, 0.5, 0.8, 1.0, 1.5 and 2.0 mM IPTG, respectively.

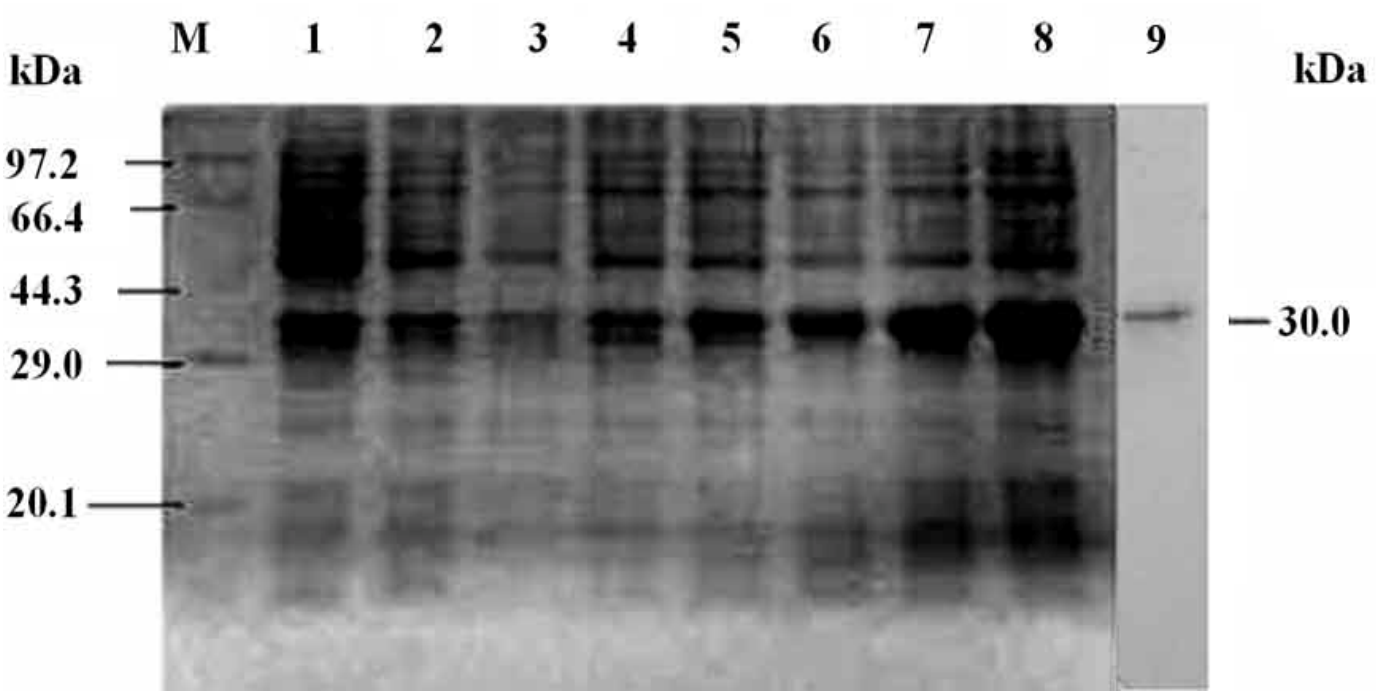

Figure 2. The effect of induction time on the expression amount of recombinant MAP30. Expression of 6×His-tagged MAP30 protein was induced by 0.5 mM IPTG. M, Marker; lane 1, negative control (BL21(DE3)); lane 2, negative control (pET-28a/BL21(DE3)); lanes 3 to 8, induced for 0, 1, 2, 3, 4 and 5 h, respectively; lane 9, purified MAP30 protein.

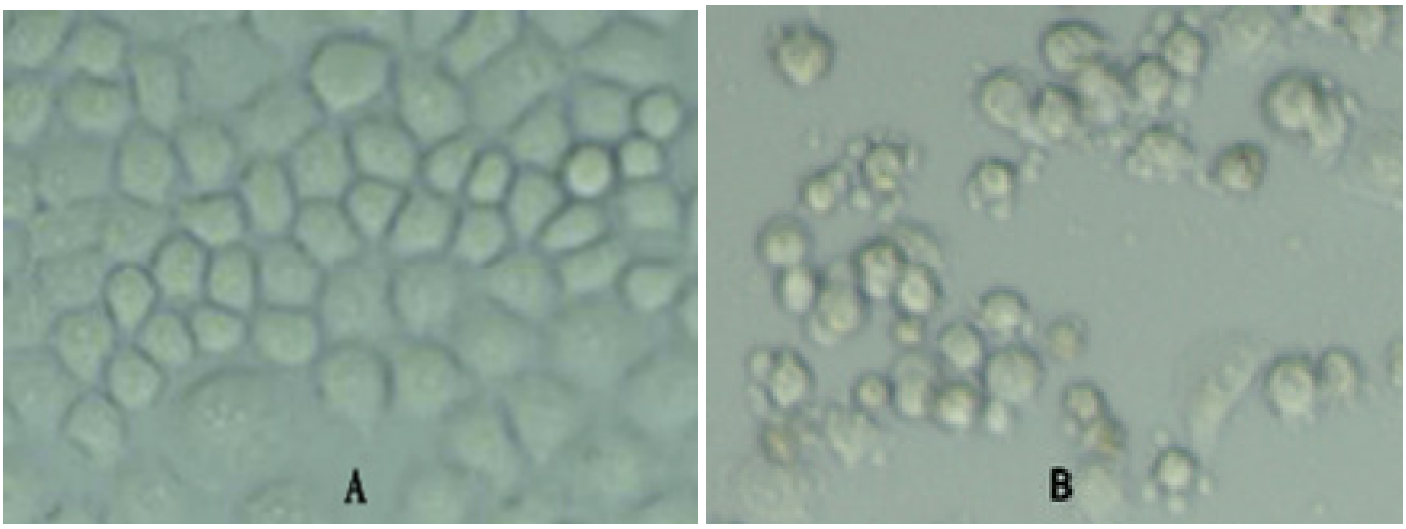

Figure 3. Morphological changes of BGC-823 cells treated by MAP30 for 48 h under light microscope. 200x (A, Control group; B, MAP30 group). When compared with the control group, the cells treated with MAP30 became round, blunt and shrink, smaller in size, had membrane blebbing, holes, cytoplasmic extrusions and formation of apoptotic bodies under light microscope.

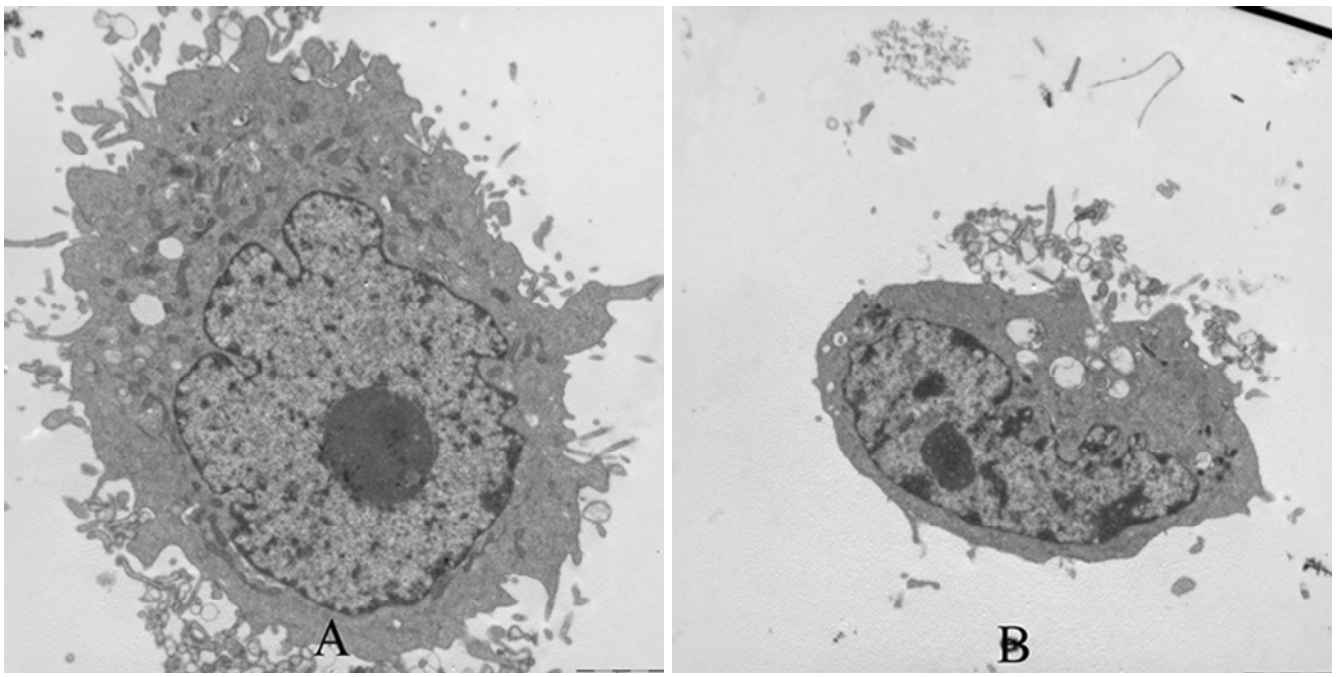

Figure 4. Morphological changes of BGC-823 cells treated with MAP30 for 48 h under electronic microscope. 10000x (A, Control group; B, MAP30 group). As shown in "B", the microvilli on the surface of the cells disappeared, cells shrink, there was cytoplasm pycnosis, nuclear membrane fold and twist, nuclear condensation, nuclear chromatin agglutination, and condensed to lump and close to membrane.

and 24.74% (48 h treated group $p<0.05$ vs. control group). All these results indicate that MAP30 could induce the BGC-823 cells apoptosis.

In recent years, several pathways leading to caspase activation and apoptosis have been elucidated, including pathways triggered by extrinsic (Fas death receptor-mediated) pathway, mitochondrion pathway and endoplasmic reticulum pathway (Choi et al., 2009; Chae et al., 2004). For zooblast, the mitochondrion pathway is the most general apoptosis mechanism and the core of

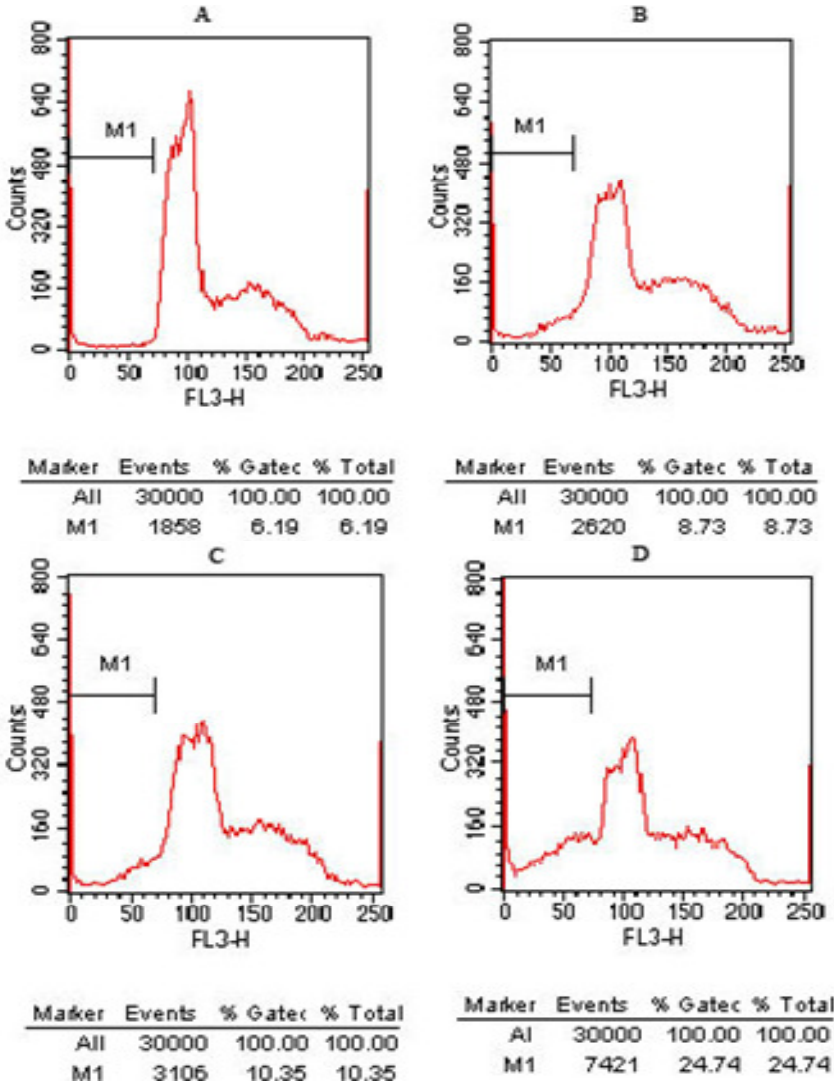

Figure 5. Cells apoptosis detected by FCM (A, Control group; B, 12 h MAP30 group; C, 24 h MAP30 group; D, 48 h MAP30 group). The subdiploid nuclear peak appeared on the left of G1 peak when the cells were treated with MAP30 and the height of the subdiploid nuclear peak elevated gradually from 12 to 48 h.

cells apoptosis (Sheng et al., 2008). Some intracellular stress signals can lead to mitochondrial outer membrane permeability (MOMP) increase (Kirkegaard and Jäättelä, 2009), which then results in ΔΨm decrease. Subsequently, Cyt C and some apoptosis inducing factors (AIF) are released from the mitochondria (De and Medema, 2008). Cyt C binds to and induces oligomerization of Apaf-1, then procaspase-9 is recruited and autoactivated. Activated caspase-9 cleaves and activates effector caspases such as caspase-3, caspase-7 and caspase-8, then cleave a variety of cellular proteins and cause cell death (Tsujimoto, 2002; Nutku et al., 2005). A key step in the intrinsic mitochondrial apoptotic pathway is the release of Cyt C from the mitochondria to activate Apaf-1, which turns on the caspase cascade. The release of Cyt C from mitochondria is usually preceded or accompanied by a reduction of ΔΨm and caspase-9. Apaf1 play a central role in the caspase cascade which is responsible for the mitochondria apoptotic process. But till now, whether the mitochondrial pathway is involved in the BGC-823 cells, apoptosis induced by MAP30 is still unknown; therefore, this study was aimed at investigating the effect of MAP30 on mitochondria pathway.

Firstly, we tested whether MAP30 could cause a loss of $\Delta\Psi_m$ by JC-1 staining. JC-1 can selectively enter into mitochondria and reversibly change color from red to green as the membrane potential decreases. As shown in Figure 6, after treated with MAP30 for 6, 12, 24 and 48 h, the red color decreased gradually and at the same time the green color increased gradually too. This indicate that MAP30 treated cells showing a majority of cells stained green due to low ΔΨm (where ΔΨm was decreased with

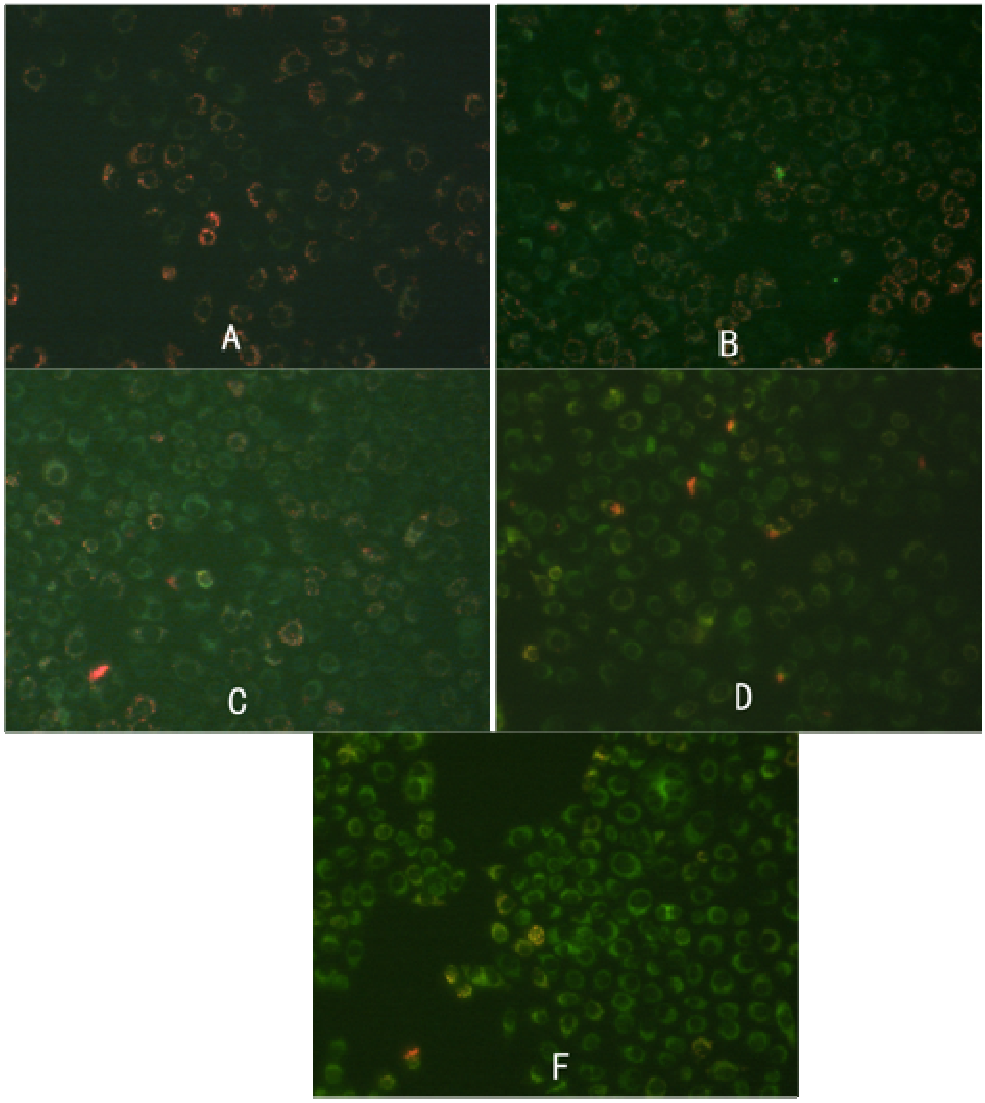

Figure 6. Effect of MAP30 on ΔΨm in BGC-823 cells under fluorescent microscopy. 200x (A, Control group; B, 6 h MAP30 group; C, 12 h MAP30 group; D, 24 h MAP30 group; F, 48 h MAP30 group). MAP30 treated cells showing that majority of cells stained green due to low ΔΨm and after treatment with MAP30 for 6, 12, 24 and 48 h, the red color decreased gradually and at the same time, the green color increased gradually too.

the effect of MAP30 in a time dependent manner). The result of ELISA showed that the release of Cyt C increased in the cells's supernate was cultured with 25 and 50 μg/ml MAP30 for 6 to 24 h. The concentration reached the peak at 24 h and then reduced after 24 h (Figure 7). The mRNA expression level of caspase-9 and Apaf1 significantly increased (Figure 8) when treated with MAP30, which indicated that mitochondria was involved in apoptosis induced by MAP30. The result of caspase-3 colorimetric assay indicated that the activities of caspase-3 were increased in the cells that were cultured with 25 and 50 μg/ml MAP30 in a time- and dose-dependent manner (Figure 9). Taken together, these data indicate that the mitochondrial-mediated apoptotic pathway played a major role in MAP30-induced BGC-823 cells apoptosis. However, in this experiment, caspase-9 mRNA reached the maximum after the cells were treated by MAP30 for 24 h, but for Apaf1 mRNA it was 48h, which indicates that the activation of caspase-9 is maybe not only dependent on the mitochondrial apoptosis pathway, but also on other factors, this requires further study.

In summary, these results demonstrate that MAP30 could induce the BGC-823 cells apoptosis *in vitro* via the mitochondrial pathway, including ΔΨm decrease, Cyt C release, Apaf-1, caspase-9 and caspase-3 activation. As we know, the different apoptosis pathways were not isolated, but intercommunicated and they developed into a complex network, which was named "cross talk" (Basu

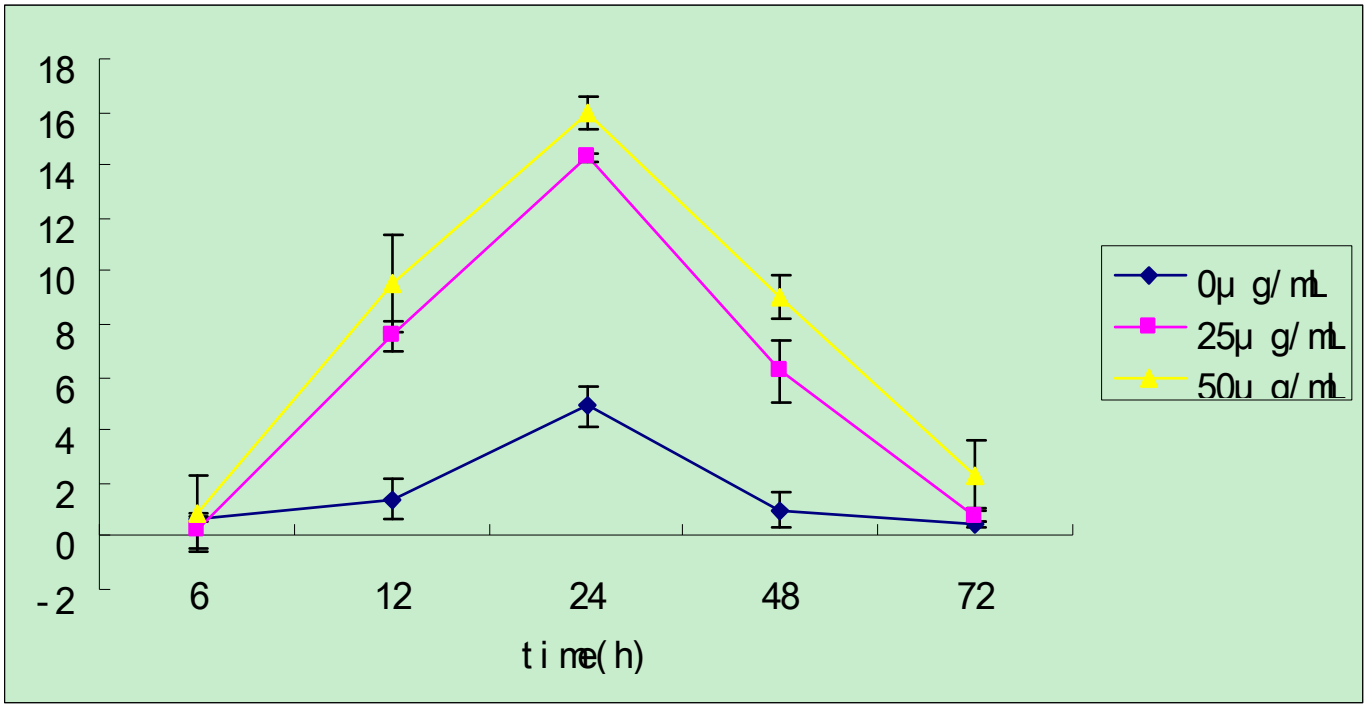

Figure 7. Effects of MAP30 on Cyt C of BGC-823 cells *in vitro*. The concentration of Cyt C reached the peak at 24 h and then reduced after 24 h. MAP30 group $p<0.05$ vs. control group at 24 h.

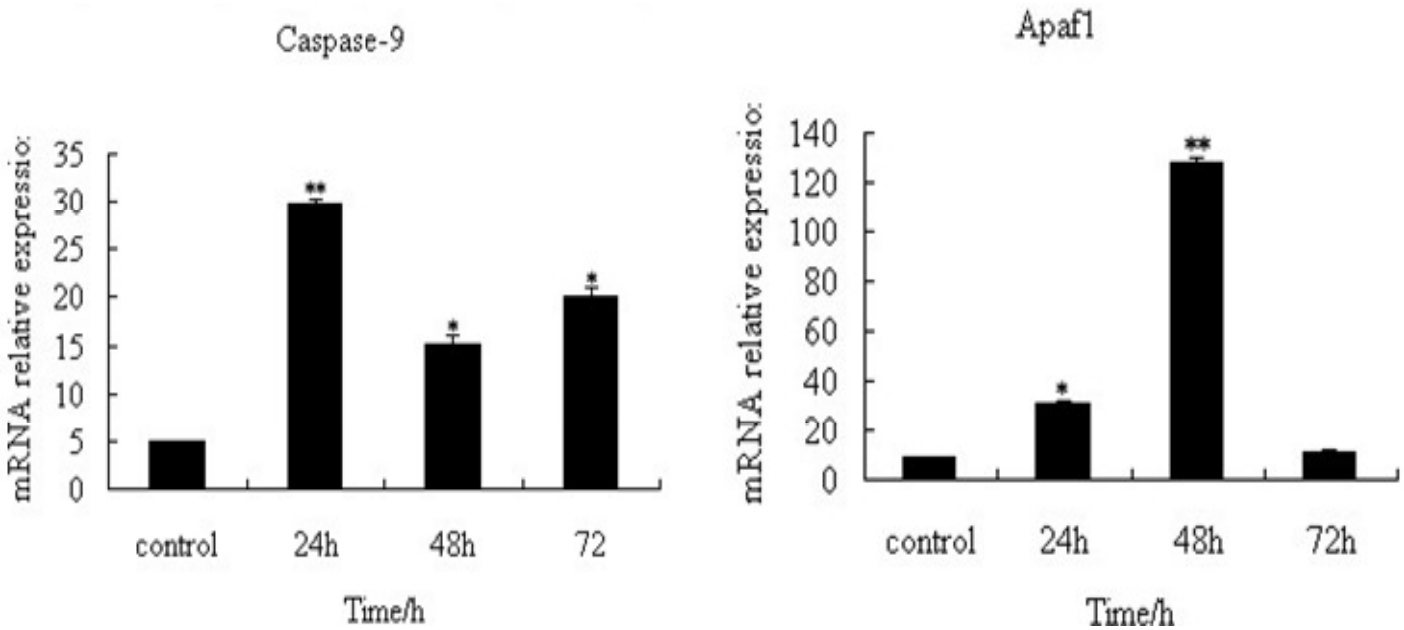

Figure 8. Time course of apoptosis-related mRNA expression by real-time RT-PCR analysis after treatment with 30 μg/ml MAP30. The mRNA expression levels of caspase-9(A) and Apaf1 (B) were quantified and normalized in each group with GAPDH. Results shown are representative of three independent experiments. *$p<0.05$, **$p<0.01$ compared to control, respectively.

et al., 2009; Kandasamy et al., 2003; Nutt et al., 2002). So, in the next study, the relationship between different apoptosis pathways will be shown.

ACKNOWLEDGEMENTS

This work was supported by grants from the National

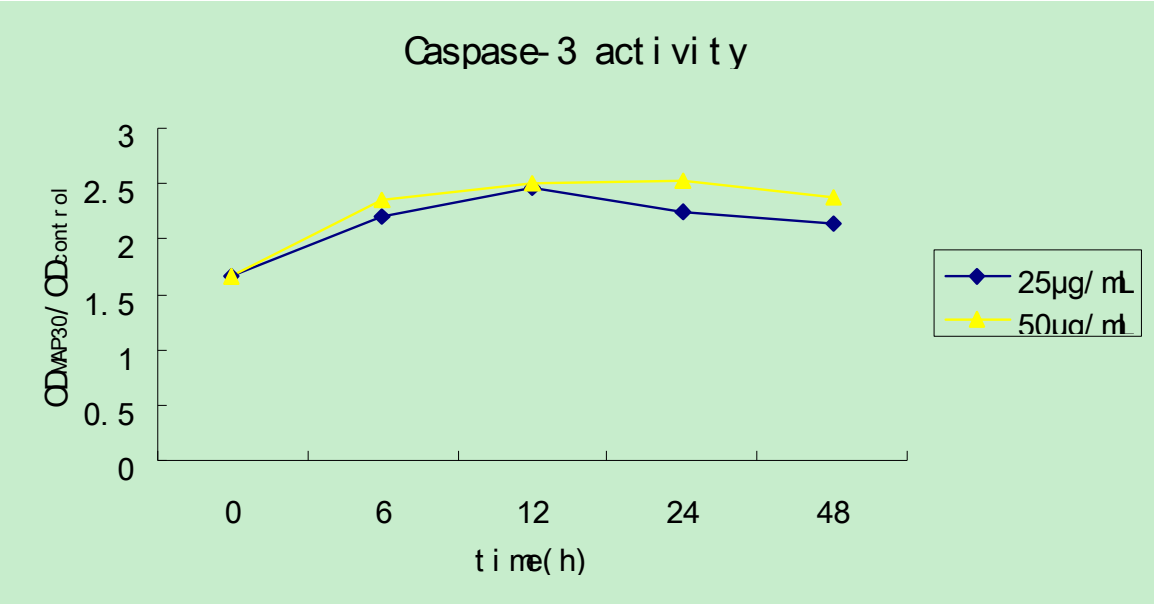

Figure 9. Effects of MAP30 on caspase-3 activity of BGC-823 cells *in vitro*. The activity of caspase-3 increased gradually after treated with 25 μg/ml MAP30 and reached the peak at 12 h and then reduced after 12 h. Otherwise, the activity of caspase-3 increased gradually after been treated with 50 μg/ml MAP30 and reached the peak at 24 h and then reduced after 24 h. For one certain concentration, $p<0.05$ vs. different time, and vice versa, that is for one certain time, $p<0.05$ vs. different concentration.

Natural Science Foundation of China (no. 30870096) and the Natural Science Foundation for College in Jiangsu Province (08KJB310001).

REFERENCES

Anonymous (2007). Momordica charantia (Bitter melon). Altern. Med. Rev. 12(4): 360-363.

Arazi T, Lee Huang P, Huang PL, Zhang L, Moshe Shiboleth Y, Gal-On A, Lee-Huang S (2002). Production of antiviral and antitumor proteins MAP30 and GAP31 in cucurbits using the plant virus vector ZYMV-AGII. Biochem. Biophys. Res. Commun. 292(2): 441-448.

Basu S, Harfouche R, Soni S, Chimote G, Mashelkar RA, Sengupta S (2009). Nanoparticle-mediated targeting of MAPK signaling predisposes tumor to chemotherapy. Proc. Natl. Acad. Sci. U.S.A. 106(19): 7957-7961.

Chae HJ, Yang SK, Kim DS, Kim HM, Chae SW, Keum KS, Kim HR (2004). Ge-Jee-Bok-Ryung-Hwan induces apoptosis in human cervical carcinoma HeLa cells--an endoplasmic reticulum stress pathway--. Life Sci. 75(25): 2997-3016.

Choi EJ, Ahn WS, Bae SM (2009). Equol induces apoptosis through cytochrome c-mediated caspases cascade in human breast cancer MDA-MB-453 cells. Chem-Biol. Interact. 177(1): 7-11.

De Bruin EC, Medema JP (2008). Apoptosis and non-apoptotic deaths in cancer development and treatment response. Cancer Treat. Rev., 34(8): 737-749.

Fulda S, Debatin KM (2006). Extrinsic versus intrinsic apoptosis pathways in anticancer chemotherapy. Oncogene, 25(34): 4798-4811.

Huang PL, Sun Y, Chen HC, Kung HF, Lee-Huang S (1999). Proteolytic fragments of anti-HIV and anti-tumor proteins MAP30 and GAP31 are biologically active. Biochem. Biophys. Res. Commun. 262(3): 615-623.

Kandasamy K, Srinivasula SM, Alnemri ES, Thompson CB, Korsmeyer SJ, Bryant JL, Srivastava RK (2003). Involvement of proapoptotic molecules Bax and Bak in tumor necrosis factor-related apoptosis-inducing ligand (TRAIL)-induced mitochondrial disruption and apoptosis: differential regulation of cytochrome c and Smac/DIABLO release. Cancer Res. 63(7):1712-1721.

Kirkegaard T, Jäättelä M (2009). Lysosomal involvement in cell death and cancer. Biochim. Biophys. Acta. 1793(4): 746-754.

Lee-Huang S, Huang PL, Chen HC, Huang PL, Bourinbaiar A, Huang HI, Kung HF (1995). Anti-HIV and anti-tumor activities of recombinant MAP30 from bitter melon. Gene. 161(2): 151-156.

Lee-Huang S, Huang PL, Sun Y, Chen HC, Kung HF, Huang PL, Murphy WJ (2000). Inhibition of MDA-MB-231 human breast tumor xenografts and HER2 expression by anti-tumor agents GAP31 and MAP30. Anticancer Res. 20(2A): 653-659.

Nutku E, Hudson SA, Bochner BS (2005). Mechanism of Siglec-8-induced human eosinophil apoptosis: role of caspases and mitochondrial injury. Biochem. Biophys. Res. Commun. 336(3): 918–924.

Nutt LK, Pataer A, Pahler J, Fang B, Roth J, McConkey DJ, Swisher SG (2002). Bax and Bak promote apoptosis by modulating endoplasmic reticular and mitochondrial Ca2+ stores. J .Biol. Chem. 277(11): 9219-9225.

Schreiber CA, Wan L, Sun Y, Lu L, Krey LC, Lee-Huang S (1999). The antiviral agents, MAP30 and GAP31, are not toxic to human spermatozoa and may be useful in preventing the sexual transmission of human immunodeficiency virus type 1. Fertil. Steril. 72(4): 686-690.

Sheng X, Sun Y, Yin Y, Chen T, Xu Q (2008). Cirsilineol inhibits proliferation of cancer cells by inducing apoptosis via mitochondrial pathway. J. Pharm. Pharmacol. 60(11): 1523-1529.

Tsujimoto Y (2002). Bcl-2 family of proteins: life-or-death switch in mitochondria. Biosci. Rep. 22(1): 47-58.